

学位論文

Significance of Tsukushi in lung cancer
(肺癌における Tsukushi の意義)

山田 竜也
Tatsuya Yamada

熊本大学大学院医学教育部博士課程医学専攻呼吸器外科学

指導教員

鈴木 実 教授
熊本大学大学院医学教育部博士課程医学専攻呼吸器外科学

伊藤 隆明 教授
熊本大学大学院医学教育部博士課程医学専攻機能病理学

2019年9月

学 位 論 文

論文題名 : Significance of Tsukushi in lung cancer
(肺癌における Tsukushi の意義)

著者名 : 山田 竜也
Tatsuya Yamada

指導教員名 : 鈴木 実 教授 熊本大学大学院医学教育部博士課程医学専攻呼吸器外科学
伊藤 隆明 教授 熊本大学大学院医学教育部博士課程医学専攻機能病理学

審査委員名 : 細胞情報薬理学講座 中西 宏之 教授
脳発生学講座 嶋村 健児 教授
呼吸器内科学講座 坂上 拓郎 教授
細胞病理学講座 菰原 義弘 准教授

2019年9月

Title: Significance of Tsukushi in lung cancer

Authors: Tatsuya Yamada^{1,2}, Kunimasa Ohta³, Yamato Motooka^{1,2}, Kosuke Fujino^{1,2}, Shinji Kudoh¹,
Yuki Tenjin^{1,4}, Younosuke Sato¹, Akira Matsuo¹, Koei Ikeda², Makoto Suzuki², and Takaaki Ito¹

Affiliations

¹ Departments of Pathology and Experimental Medicine, ² Thoracic Surgery, ³ Developmental Neurobiology, and ⁴ Respiratory Medicine, Kumamoto University, Graduate School of Medical Sciences, Honjo 1-1-1, Chuo-ku, Kumamoto 860-8556, Japan.

Corresponding author:

Takaaki Ito, M.D., D.M.Sc., Department of Pathology and Experimental Medicine, Kumamoto University, Graduate School of Medical Sciences, Honjo 1-1-1, Chuo-ku, Kumamoto 860-8556, Japan.

takaito@kumamoto-u.ac.jp

Keywords

Tsukushi, small leucine-rich repeat proteoglycan, epithelial–mesenchymal transition, cell proliferation, lung cancer

Abstract

Objectives

Tsukushi (TSK), a member of the small leucine-rich repeat proteoglycan (SLRP) family, plays multifunctional roles by interacting with signaling molecules during development. However, the role of TSK in cancer remains unknown. The aim of the present study was to investigate the biological significance of TSK in lung cancer.

Materials and methods

Immunohistochemistry of lung cancer tissues and reverse transcription polymerase chain reaction (PCR) of lung cancer cell lines were carried out to detect TSK. Then, RNA sequence analysis, Gene Ontology analysis, quantitative real-time PCR, western blotting, cell counting assay, invasion assays, and xenograft studies were done in a human lung adenocarcinoma cell line, H1975 with modification of TSK expression levels, in order to investigate its biological roles, in particular epithelial–mesenchymal transition (EMT) and proliferation.

Results

TSK was found to be highly expressed in lung cancer tissues and cell lines. Modification of TSK expression levels in H1975 resulted in changes in molecules related to EMT, including cadherin-1, snail family transcriptional repressor 1, snail family transcriptional repressor 2, and vimentin. The results of cell counting and xenograft assays showed that TSK promotes cell proliferation.

Conclusions

In lung cancer cells, TSK is expressed more highly than the other SLRPs family members, and regulates the EMT and proliferation. Thus, TSK may be a key coordinator of multiple pathways and an important structural element in the lung cancer microenvironment.

1. Introduction

The survival rate of lung cancer patients has been improving steadily. This improvement is directly tied to changes in therapy that have occurred during the past two decades, with the development of new therapies, such as tyrosine kinase inhibitors and immune checkpoint inhibitor therapy [1]. However, lung cancer is still the leading cause of cancer-related mortality worldwide [2]. The identification of new therapeutic targets will be required to further improve survival rates.

Previously, we reported the significance of Tsukushi (TSK), a member of the small leucine-rich repeat proteoglycan (SLRP) family, in development and its multifunctional roles by interacting with signaling molecules [3]. TSK binds directly to bone morphogenetic protein 4 (BMP4) to function as a BMP4 antagonist [4], modifies Notch signaling through binding delta-like 1 [5], inhibits Wnt signaling by binding to Frizzled 4 [6], and regulates transforming growth factor- β 1 (TGF- β 1) signaling through binding to TGF- β 1 [7, 8]. Thus, TSK may be a key coordinator of multiple cell signaling pathways in various tissues in both normal and pathological conditions. There have been few reports examining TSK in human cancers. Previous studies have shown that TSK increases in breast cancer with 17 β estradiol treatment [9] and in osteosarcoma with vitamin K2 treatment [10]. In spite of possible diverse potentials of TSK, there have been no reports on the functional analysis of TSK in human cancers.

For decades, decorin (DCN) and biglycan (BGN), which are other SLRPs, have been considered

as structural elements of the extracellular matrix (ECM) [11]. DCN is an inhibitor of epidermal growth factor receptor (EGFR) and hepatocyte growth factor signaling [12]. DCN also acts as a partial agonist for vascular endothelial growth factor receptor 2 [13] and bound Toll-like receptor (TLR) 2 and 4 as damage-associated molecular patterns [14]. As a result, DCN may be associated with angiogenesis, autophagy, and inflammation, and work in tumor suppression [11]. On the other hand, BGN binds TLR 2 and 4, and activates p38, extracellular signal-regulated kinase (ERK), and nuclear factor kappa-light-chain-enhancer of activated B cells (NF- κ B) signaling pathways [11, 15]. Then BGN stimulates the generation of pro-inflammatory cytokines, NADPH oxidases [16], reactive oxygen species [17], hypoxia-inducible factor-2 α , erythropoietin [18], and vascular endothelial growth factor [19], which are crucial mediators of inflammation and angiogenesis in cancer development. As a result, BGN is involved in angiogenesis and inflammation, and promotes tumorigenesis. [11]. SLRP family members crosstalk with each other in the extracellular matrix [20]. These previous studies suggested that TSK might serve as a material element in the extracellular matrix and be related to cancer development.

Metastasis determines cancer mortality. Epithelial–mesenchymal transition (EMT) is recognized as a crucial event in cancer progression and metastasis [21]. TGF- β 1 signaling plays an important role in various cancer cell behaviors inducing EMT [22]. As well as TSK [7,8], DCN and BGN are reported to bind to TGF- β 1 [23] and to affect EMT [24, 25]. TSK is supposed to be an important

molecule to modify EMT in cancer cells.

The aim of this study was to detect TSK in lung cancer tissues and cells, and to try to clarify its biological significance in them. First, we examined TSK expression in surgically resected lung cancer tissues by immunohistochemistry (IHC), and in various human lung cell lines using reverse transcription polymerase chain reaction (RT-PCR). Then, to modify TSK expression, we used plasmid DNA transfection and clustered regularly interspaced short palindromic repeat (CRISPR)/CRISPR-associated proteins 9 (Cas9) in an adenocarcinoma cell line, and, after RNA sequence analysis of lung cancer cells with various TSK expression levels, quantitative real-time polymerase chain reaction (qRT-PCR) and western blotting (WB) analysis were performed to clarify role of TSK in lung cancer. Moreover, TSK-transfected adenocarcinoma cells were implanted into immunocompromised mice, and the role of TSK in the growth of lung cancer was studied.

2. Material and methods

2.1. Cell lines

Three adenocarcinoma (ADC) cell lines (A549, H358, and H1975), three squamous cell carcinoma (SCC) cell lines (H226, H2170, and HCC15), and four small cell lung carcinoma (SCLC) cell lines (H69, H889, SBC1, and H69AR) were used in this study. H69, H69AR, A549, H358, H1975, H226, and H2170 were purchased from ATCC (Manassas, VA, USA), and SBC1 was purchased from Japan Collection of Research Bioresources Cell Bank (Osaka, Japan). HCC15 was a generous gift from Dr. Adi F. Gazdar (University of Texas Southwestern Medical Center, Dallas, TX).

2.2. Tissue samples

Tissue samples of ADC (n=30), SCC (n=17) and SCLC (n=15), resected at the Department of Thoracic Surgery of Kumamoto University Hospital were obtained from 62 patients for the following studies. A histological diagnosis of the samples was made in accordance with World Health Organization criteria [26]. These sections were used for IHC. The study followed the guidelines of the Ethics Committee of Kumamoto University.

2.3 IHC

Formalin-fixed, paraffin-embedded specimens were cut into sections (3 μ m thick) and mounted onto

MAS-GP-coated slides (Matsunami Glass Ind, Osaka, Japan). After being deparaffinized and rehydrated, the sections were heated using an autoclave in 0.01 mol/L citrate buffer (pH 6.0 or 7.0) for antigen retrieval. The sections were incubated with 0.3% H₂O₂ in absolute methanol for 20 minutes to block endogenous peroxidase activity. Then, the sections were incubated with skimmed milk for 30 minutes to block non-specific staining. After this blocking step, the sections were incubated with the primary antibodies (Supplemental Table 1) at 4°C overnight. This was followed by sequential 1-hour incubations with the secondary antibodies (En Vision+System-HRP-Labeled polymer; Dako, Glostrup, Denmark) and visualization with liquid DAB+substrate Chromogen System (Dako). All slides were counterstained with hematoxylin for 30 seconds before being dehydrated and mounted. The specificity of immunolabelling of each antibody was tested by using normal mouse IgG (Santa Cruz Biotechnology, Santa Cruz, CA), and normal rabbit IgG (Santa Cruz Biotechnology).

2.4 WB analysis

Cultured cells were prepared for WB analysis, as described previously [27]. A list of the primary antibodies used is shown in Supplemental Table 1. The membrane was then washed and incubated with the respective secondary antibodies conjugated with horseradish peroxidase (Cell Signaling, Danvers, MA) for 1 hour, and the immunocomplex was visualized with chemiluminescence

substrate (Amersham Pharmacia Biotech, Buckinghamshire, UK).

2.5 RT-PCR and qRT-PCR

Total RNA was isolated using an RNeasy Mini Kit (Qiagen, Hilden, Germany) and cDNA was produced using ReverTraAce qPCR RT-Kit (Toyobo, Osaka, Japan). RT-PCR was conducted in accordance with the standard protocol for TAKARA Ex taq (TAKARA Bio, Shiga, Japan) and DNA amplification was performed using a Mastercycler® nexus (Eppendorf, Hamburg, Germany). The cycling conditions were as follows: one cycle at 95°C for 5 minutes, followed by 28 cycles at 95°C for 30 seconds, 60°C for 30 seconds, and 72°C for 35 seconds. The amplification products were separated by 1.5% agarose gel electrophoresis and were analyzed using an ultraviolet transilluminator. qRT-PCR was conducted according to the standard protocol of SYBR fast qPCR Mix (TAKARA Bio) on a LiteCycler Nano (Roche, Penzberg, Germany). Data were obtained from triplicate reactions. The means and standard deviation (SD) of the copy number were normalized to the value for glyceraldehyde-3-phosphate dehydrogenase (GAPDH) mRNA. A list of the specific primers is shown in Supplemental Table 2.

2.6 Plasmid construction and transfection

TSK-expressing vector

To construct p3×FLAG-CMV-14-TSK (Sigma Aldrich, Oakville, Canada), human TSK was PCR amplified, and cloned into the p3×FLAG-CMV-14. The plasmid was transfected by Lipofectamine 3000 (Thermo Fisher Scientific, Carlsbad, CA) into cells at subconfluency. After 48 hours, the transfected cells were treated with 500 µg/mL G418 (Clontech, Mountain View, CA) for selection of stably transfected cells.

TSK-knockout vector

Genome editing using CRISPR/ Cas9 was used for knockout of TSK gene in the H1975 cell line. pSpCas9(BB)-2A-Puro(px459) was obtained from Addgene (Cambridge, MA) [28]. The sgRNA target sequences of TSK were as follows: CTT CCC CGG GTG CCA ATG CG and GGC ACT ACA CGT GGA CCT CT. These plasmids were co-transfected with Lipofectamine 3000 (Thermo Fisher Scientific) into the cells at subconfluency. After 48 hours, the transfected cells were treated with 1 µg/mL puromycin (Clontech) for selection of stably transfected cells.

2.7 Cell counting assay

Mock transfected H1975 cells and TSK-overexpressed H1975 cells (TSK-OE) line were seeded at equivalent densities (1.0×10^5 cells/well) in 6-well plates. After 24, 48, and 72 hours, the cells were trypsinized and then counted. The experiments were repeated in triplicate to confirm reproducibility.

2.8 Cell invasion assay

Matrigel invasion assays were conducted in accordance with the standard protocol of the Corning Matrigel Invasion Chamber (Bio coat, Horsham, PA). The mock and TSK-OE line (5.0×10^4 cells) were plated onto each chamber in serum-free growth medium. Chambers were placed in wells containing growth medium with 10% FBS. After 24 hours incubation at 37°C in a CO₂ incubator, the Matrigel membranes were collected and stained with Diff-Quik (Sysmex, Hyogo, Japan). The number of cells that migrated to the undersurface of the membrane was examined using a microscope, photographed, and counted in five randomly selected microscopic fields.

2.9 RNA sequence analysis

RNA sequence analysis was performed by the Liaison Laboratory Research Promotion Center (LILA) (Kumamoto University) as follows. Total RNA was isolated from cultured cells, including the mock transfected H1975 cell (p3×FLAG-CMV-14 and pSpCas9(BB)-2A-Puro(px459)), TSK-OE, and TSK knockout H1975 cell (TSK-KO) line, using an RNeasy Mini Kit (Qiagen). A 2100 Bioanalyzer (Agilent, Santa Clara, CA) was used to detect the concentration and purity of total RNA. All samples with an RNA integrity number (RIN) >7.5 were used for sequencing. Nextseq 500

(Illumina, San Diego, CA) were used to analyze, the data was converted to Fastq files. The quality control of the data was performed by FastQC. Then, the filtered reads were used to mapped to the UCSC hg19 genome reference genome using HISAT2 2.1.0. Fragments per kilobase of exon per million reads mapped (FPKM) values were calculated using Cufflinks. Significant genes were extract by cuffdiff ($p < 0.05$).

2.10 Gene ontology (GO) analysis

GO annotation and classification were based on three categories, including biological process, molecular function, and cellular component. The Database for Annotation, Visualization, and Integrated Discovery 6.7 (DAVID 6.7, <http://www.david.niaid.nih.gov>) was used for GO analysis [29]. The gene list contained significant genes in the RNA sequence analysis. To visualize the key molecular functions and biological processes, the DAVID online database was used. $p < 0.05$ was regarded as the cut-off criterion with statistic difference.

2.11 Tumor xenograft growth and histopathological evaluation

A total of 1.0×10^6 cells each of the mock transfected and TSK-OE lines were injected subcutaneously into the back of mice [Rag2^{-/-}:Jak3^{-/-} mice; a generous gift from Prof. Seiji Okada (Kumamoto University)]. Twenty days after the first injection, the tumor were removed and

measured. The samples were fixed with phosphate-buffered 4% paraformaldehyde solution and embedded in paraffin. Tissue sections were stained with hematoxylin and eosin, and additional sections were used for immunohistochemical analysis. All animal experiments were conducted in accordance with the guidelines of Animal Care and Use Committee of Kumamoto University.

2.12. Statistical analysis

All data were obtained from independent experiments, and were expressed as the means \pm SDs of triplicate determinations. The differences in the mean values between the two groups were statistically analyzed using t-test. Prism v.7 software (GraphPad Software, San Diego, CA) was used for statistical analyses. $p < 0.05$ was considered as significant.

3. Results

3.1. TSK is expressed in lung cancer tissue sections and cell lines

Surgically resected lung cancer tissues (30 ADC, 17 SCC, and 15 SCLC) were stained immunohistochemically for TSK by IHC (Figure 1A). TSK was significantly increased in tumor tissues compared with adjacent normal lung tissues. Distinct staining for TSK was observed in the cytoplasm of lung cancer cells. There was a mild tendency that TSK seemed to be more highly expressed in NSCLC than SCLC, but some SCLC cases also showed positive staining (Table 1). Next, we examined TSK expression in 10 lung cancer cell lines (three ADC, three SCC, and four SCLC) by WB. However, TSK expression was rarely detected in them (data not shown). Then, we performed RT-PCR with the lung cancer cell lines to evaluate the expression of SLRP family mRNAs, including TSK, DCN, BGN, lumican (LUM), asporin (ASPN), and podocan (PODN) (Figure 1B). The cycling conditions were 28 cycles for each gene. TSK mRNA was expressed in all the lung cancer cell lines examined. On the other hand, DCN, ASPN, and PODN mRNAs were not detected in the lung cancer cell lines examined. BGN mRNA was expressed in cell lines H226, H69, and H69AR. LUM mRNA was expressed in H358 and SCLC cell lines. Thus, TSK mRNA was expressed in more lung cancer cell lines than other SLRP mRNAs (Figure 1B).

3.2. Modification of TSK expression in H1975 adenocarcinoma cells

WB was performed to measure the TSK and Flag expression in TSK-OE clones (Figure 2A). TSK and Flag were more highly expressed in TSK-OE clone #2 than in clone #1. We selected clone #2 for further studies, including RNA sequence and qRT-PCR. FPKM levels of TSK obtained by RNA sequence and relative expression of TSK obtained by qRT-PCR in the TSK-OE clone #2 are shown in Figure 2B.

Although TSK expression was rarely detected in the lung cancer cell lines examined by WB, TSK mRNA was detected consistently by RT-PCR. RT-PCR was performed to measure the TSK mRNA levels in TSK-KO clones (Figure 2C). TSK mRNA was expressed at lower levels in TSK-KO clone #1 than the other clones (data not shown), and we selected the clone #1 for further studies, including RNA sequence and qRT-PCR. FPKM level of TSK obtained by RNA sequence and relative expression of TSK obtained by qRT-PCR in TSK-KO clone #1 is shown in Figure 2D.

3.3. RNA sequence and GO analysis

To assess global mRNA changes associated with increase or decrease of TSK gene in a lung ADC cell line, we performed RNA sequence analysis, followed by qRT-PCR to confirm changes in the expression of selected genes of interest. We found that the expression of 346 genes was significantly different between the mock transfected (p3×FLAG-CMV-14-TSK) and TSK-OE cell lines, including 233 up-regulated and 113 down-regulated genes. Then, we found that the expression

of 383 genes was significantly different between the mock transfected (pSpCas9(BB)-2A-Puro(px459)) and TSK-KO cell lines, including 284 up-regulated and 99 down-regulated genes. 94 common significantly affected genes were found, after comparing the analysis of TSK-OE and TSK-KO cell lines (Figure 3A). Among them, four genes, which were up-regulated in TSK-OE and down-regulated in TSK-KO cell lines, were detected, including proprotein convertase subtilisin/kexin type 1 inhibitor (PCSK1N), LIM, and calponin homology domains-containing protein 1 (LIMCH1), fructose-bisphosphatase 1 (FBP1), and TSK. On the other hand, 10 genes, which were down-regulated in TSK-OE and up-regulated in TSK-KO cell lines, were detected, including neuropilin 2 (NRP2), podocalyxin-like (PODXL), sulfide quinone reductase-like (SQRDL), alanyl aminopeptidase, membrane (ANPEP), neutrophil cytosolic factor 2 (NCF2), hyaluronan synthase 2 (HAS2), myosin heavy chain 16 pseudogene (MYH16), leucine-rich repeat-containing protein 8C (LRRC8C), aldehyde dehydrogenase 1 family, member A3 (ALDH1A3), and endothelin receptor type A (EDNRA) (Figure 3B).

The DAVID online bioinformatics tool was used for GO functional analysis of the significantly affected genes. The top 20 significantly enriched terms ($p < 0.05$) in molecular functions and biological processes category are presented in Supplemental Fig. 1. We paid close attention to the molecular functions, such as adhesion and proliferation. The heat maps of molecules, in regard to adhesion and proliferation functions, are presented in Supplemental Figure 2. Among the 14

significant common genes, NRP2 and PODXL are adhesion-related molecules, and PCSK1N and EDNRA are proliferation-related molecules. Meng X et al. [30] indicated that PODXL was related to TGF- β 1 signaling and played roles in adhesion. qRT-PCR analysis revealed that PODXL and TGF- β 1 were elevated in TSK-KO cells, and, in contrast, were reduced in TSK-OE cells (Figure 3C).

3.4. TSK regulates EMT in H1975 adenocarcinoma cells

First, qRT-PCR of TSK-OE was done to investigate role of TSK in EMT. Expression of snail family transcriptional repressor 1 (SNAI1), snail family transcriptional repressor 2 (SNAI2), and vimentin (VIM) was significantly reduced, and expression of cadherin-1 (CDH1) was elevated in TSK-OE. This expression pattern was similar to the results obtained by the RNA sequence analysis (Figure 4A). Moreover, WB of TSK-OE supported the significant reduction in SNAI1, SNAI2, and VIM, but induction of CDH1 by overexpression of TSK was not evident by WB (Figure 4B).

Next, qRT-PCR of TSK-KO was done to investigate role of TSK in EMT. Expression of SNAI2 and VIM was significantly elevated, but expression of SNAI1 was reduced in TSK-KO. This expression pattern was similar to the results obtained by RNA sequence analysis, except for SNAI1 (Figure 4C). When WB of the TSK-KO was performed, the induction of SNAI1, SNAI2, VIM, or CDH1 was not evident (Figure 4D). Taken together, these results suggested that TSK inhibits EMT.

To confirm whether TSK inhibits EMT, we further performed invasion assays in the mock transfected and TSK-OE cell lines. The degree of cell invasion in TSK-OE cells was clearly less than that of the mock transfected cells (mock versus TSK-OE, 56.2 ± 8.04 cell numbers/field versus 26.2 ± 3.83 cell numbers/field) (Figure 4E).

3.5. TSK is involved in cell proliferation in H1975 adenocarcinoma cells

To confirm role of TSK in cell proliferation, we performed cell counting assays in mock transfected and TSK-OE cell lines, which revealed that TSK overexpression enhanced the proliferation of H1975 cells (Figure 5A). However, mitogen-activated protein kinases (MAPKs), such as phosphorylation of ERK1/2 and p38, were reduced in TSK-OE in WB analyses (Figure 5B). Moreover, these cells were transplanted into subcutaneous tissue of immunocompromised mice to evaluate the difference in proliferation activity of the cells. The size of xenotransplanted tumors from TSK-OE was significantly larger than that of tumors from mock transfected cells (Figure 5C). In addition, the Ki67-labeling index was elevated in tumor tissues from TSK-OE, compared with those from mock transfected cells (Ki67-labeling index of the tumors from the mock transfected versus TSK-OE, $71.3 \pm 3.49\%$ versus $83.1 \pm 2.47\%$) (Figure 5D). However, MAPK expression, such as ERK1/2, was slightly reduced in xenotransplanted tumors of TSK-OE in WB analyses (Figure 5E). These results suggested that TSK overexpression enhanced cell proliferation activity without

activating MAPK signaling.

4. Discussion

The present investigation demonstrated the presence of TSK in lung cancer cells, and clarified the roles of TSK in them. We first performed IHC and RT-PCR to detect TSK in lung cancer tissues and cells. TSK was found to be more highly expressed in lung cancer tissues than in normal lung tissues, and to be more highly expressed than other SLRPs in lung cancers. Although TSK mRNA levels were high in lung cancer cell lines, TSK protein was not always detected in them by WB. It may be considered that the reason for the discrepancy between WB and RT-PCR may be attributed to the lower sensitivity of the antibody for TSK and to extracellular secretion of TSK protein. [4]. Bozoky et al. [31] reported a marked reduction in DCN expression within the stroma of many solid tumors. They suggested that DCN was abundantly secreted, deposited in the normal connective tissue, and disappear consistently from the tumor microenvironment. On the other hand, another study showed that stromal DCN expression was increased in cancer cells [32]. BGN expression was increased in a variety of human malignancies, such as colon cancer [33], intrahepatic cholangiocarcinoma [34], and esophageal squamous cell carcinoma [35]. Moreover, there were reports that BGN expression levels were higher in tumor endothelial cells than in normal endothelial cells [36, 37]. Considering these reports about other SLRP family members and the present study, it is suggested that various SLRPs are present in some cancer tissues, and TSK may be one of the most important SLRPs and to function in lung cancer tissues and cells.

EMT is characterized by changes in specific molecules, such as CDH1, SNAI1, SNAI2, and VIM, followed by the loss of cell–cell junctions, cell–matrix adhesion, or modulation of polarity, resulting in increasing migration and invasion ability [38, 39]. TGF- β 1 signaling plays a pivotal role in regulating EMT [22]. There are some reports regarding the interaction of DCN and BGN with TGF- β 1. TGF- β 1 inhibits transcription of DCN and induces transcription of BGN [40]. Moreover, TGF- β 1 was increased in DCN knockout fetal mice and decreased in BGN knockout fetal mice [41]. Recent investigations demonstrated that the invasion ability of DCN-overexpressing trophoblast cells was significantly lower than controls [25]. On the other hand, the invasion ability of BGN knockdown endometrial cancer cells was significantly lower than controls [42]. Although there are still many unclear points regarding the interaction of DCN and BGN with TGF- β 1, it is quite possible that the interaction of DCN and BGN with TGF- β 1 regulates EMT. We found that TSK overexpression in a lung ADC cell line inhibited expression of SNAI1, SNAI2, and VIM, and TSK knockout in the cell line induced the expression of SNAI2 and VIM. According to these molecular modifications, TSK led to the inhibition of EMT. Little was known previously about the effect of TSK on EMT in lung cancer. Previously, we reported that TGF- β 1 was significantly more highly expressed in TSK knockout mice in comparison with wild-type mice [8]. In the present study, TGF- β 1 was significantly more highly expressed in TSK-KO cells, and expression was reduced in TSK-OE cells in comparison to each in mock transfected cells. In addition, expression of PODXL

showed similar results. Because PODXL also plays a pivotal role in regulating EMT [30], it is possible that the interaction of TSK regulates EMT through controlling TGF- β 1 and PODXL.

Although little was known previously about the role of TSK in the proliferation of human neoplasms, we found that TSK expression promotes cell proliferation of lung cancer cells. In the present study, xenotransplanted tumors from TSK-OE cells were significantly larger than those from mock transfected cells, and cell growth of TSK-OE cells was also significantly faster than mock transfected cells *in vitro*. It has been reported that DCN overexpression inhibited cell proliferation [43], whereas BGN overexpression enhanced cell proliferation [44]. DCN interacts with EGFR and induces p21-mediated cell cycle arrest and apoptosis [11, 45]. Then, DCN interacts with Met and attenuates of β -catenin and Myc signaling, which inhibits tumor growth [11, 46]. BGN interacts with TLR2 and 4, and activates the NF- κ B and MAPK pathways, which leads to cancer progression due to increased tumor cell proliferation, resistance to apoptosis, and increased production of growth factors [11, 19, 47]. It has also been reported that TGF- β 1 not only regulates EMT but also suppresses proliferation [48, 49]. It is possible that the reduction in TGF- β 1 promotes proliferation in TSK-OE cells. TSK is considered to interact with several pathways, but the mechanism by which TSK induces proliferation activity has not been clarified. A limitation of our study was that we focused on only the H1975 cell line. For further studies, we consider that we should evaluate the possible association of EMT and proliferation in other cell lines. Then, we need to clarify how TSK

interacts with the WNT, Notch, BMP4, and TGF- β 1 signaling pathways.

Conclusion

In the present study, RNA sequence analysis provided extensive information to investigate the role of TSK in lung cancer. For the first time, we performed functional analysis of TSK in human cancers. In lung cancer cells, TSK is more highly expressed than the other SLRPs examined, and it regulates EMT and proliferation in cancer cells. Thus, TSK may be a key coordinator of multiple pathways and an important structural element in the lung cancer microenvironment.

Conflict of interest

The authors declare no conflict of interest.

Acknowledgments

We thank Ms. Motoko Kagayama and Ms. Takako Maeda for technical assistance; and Mr. Shingo Usuki, Mr. Naoki Tani, and the staff of the LILA for technical support; the Institute of Molecular Embryology and Genetics, Kumamoto University, for help with RNA sequencing and Proteomics analyses. This study was supported in part by the program of the Joint Usage/Research Center for Developmental Medicine, Institute of Molecular Embryology and Genetics, Kumamoto

University.

References

1. Heymach J, Krilov L, Alberg A, Baxter N, Chang SM, Corcoran R, Dale W, DeMichele A, Magid Diefenbach CS, Dreicer R, Epstein AS, Gillison ML, Graham DL, Jones J, Ko AH, Lopez AM, Maki RG, Rodriguez-Galindo C, Schilsky RL, Sznol M, Westin SN, Burstein H. Clinical cancer advances 2018: annual report on progress against cancer from the American Society of Clinical Oncology. *J Clin Oncol.* 2018; 36: 1020-1044.
2. Siegel RL, Miller KD, Jemal A. Cancer statistics, 2018. *CA Cancer J Clin.* 2018; 68: 7-30.
3. Ahmad SAI, Anam MB, Ito N, Ohta K. Involvement of Tsukushi in diverse developmental processes. *J Cell Commun Signal.* 2018; 12: 205-210.
4. Ohta K, Lupo G, Kuriyama S, Keynes R, Holt CE, Harris WA, Tanaka H, Ohnuma SI. Tsukushi functions as an organizer inducer by inhibition of BMP activity in cooperation with chordin. *Dev Cell.* 2004; 7: 347-358.
5. Kuriyama S, Lupo G, Ohta K, Ohnuma S, Harris WA, Tanaka H. Tsukushi controls ectodermal patterning and neural crest specification in *Xenopus* by direct regulation of BMP4 and X-delta-1 activity. *Development.* 2006; 133: 75-88.
6. Ohta K, Ito A, Kuriyama S, Lupo G, Kosaka M, Ohnuma S, Nakagawa S, Tanaka H. Tsukushi functions as a Wnt signaling inhibitor by competing with Wnt2b for binding to transmembrane protein Frizzled4. *Proc Natl Acad Sci U S A.* 2011; 108: 14962-14967.

7. Niimori D, Kawano R, Felemban A, Niimori-Kita K, Tanaka H, Ihn H, Ohta K. Tsukushi controls the hair cycle by regulating TGF- β 1 signaling. *Dev Biol.* 2012; 372: 81-87.
8. Niimori D, Kawano R, Niimori-Kita K, Ihn H, Ohta K. Tsukushi is involved in the wound healing by regulating the expression of cytokines and growth factors. *J Cell Commun Signal.* 2014; 8: 173-177.
9. Charpentier AH, Bednarek AK, Daniel RL, Hawkins KA, Laflin KJ, Gaddis S, MacLeod MC, Aldaz CM. Effects of estrogen on global gene expression: identification of novel targets of estrogen action. *Cancer Res.* 2000; 60: 5977-5983.
10. Ichikawa T, Horie-Inoue K, Ikeda K, Blumberg B, Inoue S. Steroid and xenobiotic receptor SXR mediates vitamin K2-activated transcription of extracellular matrix-related genes and collagen accumulation in osteoblastic cells. *J Biol Chem.* 2006; 281: 16927-16934.
11. Schaefer L, Tredup C, Gubbiotti MA, Iozzo RV. Proteoglycan neofunctions: regulation of inflammation and autophagy in cancer biology. *FEBS J.* 2017; 284: 10-26.
12. Neill T, Painter H, Buraschi S, Owens RT, Lisanti MP, Schaefer L & Iozzo RV. Decorin antagonizes the angiogenic network. Concurrent inhibition of Met, hypoxia inducible factor-1 α and vascular endothelial growth factor A and induction of thrombospondin-1 and TIMP3. *J Biol Chem.* 2012; 287: 5492–5506.

13. Buraschi S, Neill T, Goyal A, Poluzzi C, Smythies J, Owens RT, Schaefer L, Torres A, Iozzo RV. Decorin causes autophagy in endothelial cells via Peg3. *Proc Natl Acad Sci U S A*. 2013; 110: E2582-91.
14. Merline R, Moreth K, Beckmann J, Nastase MV, Zeng-Brouwers J, Tralhão JG, Lemarchand P, Pfeilschifter J, Schaefer RM, Iozzo RV, Schaefer L. Signaling by the matrix proteoglycan decorin controls inflammation and cancer through PDCD4 and MicroRNA-21. *Sci Signal*. 2011; 4: ra75.
15. Schaefer L, Babelova A, Kiss E, Hausser H-J, Baliova M, Krzyzankova M, Marsche G, Young MF, Mihalik D, Götte M, Malle E, Schaefer RM, Gröne H-J. The matrix component biglycan is proinflammatory and signals through toll-like receptors 4 and 2 in macrophages. *J Clin Invest*. 2005; 115: 2223–2233.
16. Hsieh LT, Frey H, Nastase MV, Tredup C, Hoffmann A, Poluzzi C, Zeng-Brouwers J, Manon-Jensen T, Schröder K, Brandes RP, Iozzo RV, Schaefer L. Bimodal role of NADPH oxidases in the regulation of biglycan-triggered IL-1 β synthesis. *Matrix Biol*. 2016; 49: 61-81.
17. Babelova A, Moreth K, Tsalastra-Greul W, Zeng-Brouwers J, Eickelberg O, Young MF, Bruckner P, Pfeilschifter J, Schaefer RM, Gröne HJ, Schaefer L. Biglycan, a danger signal that activates the NLRP3 inflammasome via Toll-like and P2X receptors. *J Biol Chem*. 2009; 284: 24035-24048.

18. Frey H, Moreth K, Hsieh LT, Zeng - Brouwers J, Rathkolb B, Fuchs H, Gailus - Durner V, Iozzo RV. A novel biological function of soluble biglycan: Induction of erythropoietin production and polycythemia. *Glycoconj J.* 2017; 34: 393-404.
19. Hu L, Zang MD, Wang HX, Li JF, Su LP, Yan M, Li C, Yang QM, Liu BY, Zhu ZG. Biglycan stimulates VEGF expression in endothelial cells by activating the TLR signaling pathway. *Mol Oncol* 2016; 10: 1473-1484.
20. Kristin M, Renato V. I, Liliana S. Small leucine-rich proteoglycans orchestrate receptor crosstalk during inflammation. *Cell Cycle.* 2012; 11: 2084–2091.
21. Thiery J.P., Acloque H., Huang R.Y., Nieto M.A. Epithelial–mesenchymal transitions in development and disease. *Cell.* 2009; 139: 871–890.
22. Xu J, Lamouille S, Derynck R. TGF-beta-induced epithelial to mesenchymal transition. *Cell Res.* 2009; 19: 156-172.
23. Hildebrand A, Romarís M, Rasmussen LM, Heinegard D, Twardzik DR, Border WA, Ruoslahti E. Interaction of the small interstitial proteoglycans biglycan, decorin and fibromodulin with transforming growth factor beta. *Biochem J.* 1994; 302: 527-34.
24. Li H, Zhong A, Li S, Meng X, Wang X, Xu F, Lai M. The integrated pathway of TGFβ/Snail with TNFα/NFκB may facilitate the tumor-stroma interaction in the EMT process and colorectal cancer prognosis. *Sci Rep.* 2017; 7: 4915.

25. Zou Y, Yu X, Lu J, Jiang Z, Zuo Q, Fan M, Huang S, Sun L. Decorin-Mediated Inhibition of Human Trophoblast Cells Proliferation, Migration, and Invasion and Promotion of Apoptosis In Vitro. *Biomed Res Int.* 2015; 2015: 201629.
26. Travis, WD, Brambilla, E, Burke, AP, Marx, A, and Nicholson, AG. WHO Classification of Tumours of the Lung, Pleura, Thymus and Heart. International Agency for Research on Cancer, Lyon; 2015
27. Motooka Y, Fujino K, Sato Y, Kudoh S, Suzuki M, and Ito T. Pathology of Notch2 in lung cancer. *Pathology.* 2017; 49, 486-493.
28. Ran F, Hsu PD, Wright J, Agarwala V, Scott DA, and Zhang F. Genome engineering using the CRSPR-Cas9 system. *Nat Protoc.* 2013; 8: 2281-2308
29. Huang DW, Sherman BT, Lempicki RA. Systematic and integrative analysis of large gene lists using DAVID Bioinformatics Resources. *Nature Protoc.* 2009; 4: 44-57.
30. Meng X, Ezzati P, Wilkins JA. Requirement of podocalyxin in TGF-beta induced epithelial mesenchymal transition. *PLoS One.* 2011; 6: e18715.
31. Bozoky B, Savchenko A, Guven H, Ponten F, Klein G, Szekely L. Decreased decorin expression in the tumor microenvironment. *Cancer Med.* 2014; 3: 485-491.

32. Brown LF, Guidi AJ, Schnitt SJ, Van De Water L, Iruela-Arispe ML, Yeo TK, Tognazzi K, Dvorak HF. Vascular stroma formation in carcinoma in situ, invasive carcinoma, and metastatic carcinoma of the breast. *Clin Cancer Res.* 1999; 5: 1041-1056.
33. Mikula M, Rubel T, Karczmariski J, Goryca K, Dadlez M, Ostrowski J. Integrating proteomic and transcriptomic high-throughput surveys for search of new biomarkers of colon tumors. *Funct Integr Genomics.* 2011; 11: 215–224.
34. Nishino R, Honda M, Yamashita T, Takatori H, Minato H, Zen Y, Sasaki M, Takamura H, Horimoto K, Ohta T, Nakanuma Y, Kaneko S. Identification of novel candidate tumour marker genes for intrahepatic cholangiocarcinoma. *J Hepatol.* 2008; 49: 207–216.
35. Zhu YH, Yang F, Zhang SS, Zeng TT, Xie X, Guan XY. High expression of biglycan is associated with poor prognosis in patients with esophageal squamous cell carcinoma. *Int J Clin Exp Pathol.* 2013; 6: 2497–2505.
36. Yamamoto K, Ohga N, Hida Y, Maishi N, Kawamoto T, Kitayama K, Akiyama K, Osawa t, Kondoh M, Matsuda K, Onodera Y, Fujie M, Kaga K, Hirano S, Shinohara N, Shinodoh M, Hida K. Biglycan is a specific marker and an autocrine angiogenic factor of tumour endothelial cells. *Brit J Cancer.* 2012; 106: 1214–1223.
37. Maishi N, Ohba Y, Akiyama K, Ohga N, Hamada J, Nagao-Kitamoto H, Alam MT, Yamamoto K, Kawamoto T, Inoue N, Taketomi A, Shindoh M, Hida Y, Hida K. Tumour endothelial cells in

- high metastatic tumours promote metastasis via epigenetic dysregulation of biglycan. *Sci Rep.* 2016; 6: 28039
38. Zeisberg M, Neilson EG. Biomarkers for epithelial-mesenchymal transitions. *J Clin Invest.* 2009; 119: 1429-37.
39. Liu J, Shen JX, Hu JL, Dou XW, Zhang GJ. Role of epithelial-mesenchymal transition in invasion and metastasis of breast cancers. *OA Cancer* 2013; 1: 16
40. Mauviel A, Santra M, Chen YQ, Uitto J, Iozzo RV. Transcriptional regulation of decorin gene expression. Induction by quiescence and repression by tumor necrosis factor- α . *J Biol Chem.* 1995; 270: 11692-11700.
41. Wu Z, Horgan CE, Carr O, Owens RT, Iozzo RV, Lechner BE. Biglycan and decorin differentially regulate signaling in the fetal membranes. *Matrix Biol.* 2014; 35: 266–275.
42. Sun H, Wang X, Zhang Y, Che X, Liu Z, Zhang L, Qiu C, Lv Q, Jiang J. Biglycan enhances the ability of migration and invasion in endometrial cancer. *Arch Gynecol Obstet* 2016; 293: 429-438.
43. Ma HI, Hueng DY, Shui HA, Han JM, Wang CH, Lai YH, Cheng SY, Xiao X, Chen MT, Yang YP. Intratumoral decorin gene delivery by AAV vector inhibits brain glioblastomas and prolongs survival of animals by inducing cell differentiation. *Int J Mol Sci.* 2014; 15: 4393-4414.

44. Wu B, Ma X, Zhu D, Liu Y, Sun Z, Liu S, Xue B, Du M, Yin X. Lentiviral delivery of biglycan promotes proliferation and increases osteogenic potential of bone marrow-derived mesenchymal stem cells in vitro. *J Mol Histol.* 2013; 44: 423-431.
45. Moscatello DK, Santra M, Mann DM, McQuillan DJ, Wong AJ, Iozzo RV. Decorin suppresses tumor cell growth by activating the epidermal growth factor receptor. *J Clin Invest.* 1998; 101: 406-412.
46. Buraschi S, Pal N, Tyler-Rubinstein N, Owens RT, Neill T, Iozzo RV. Decorin antagonizes Met receptor activity and downregulates β -catenin and Myc levels. *J Biol Chem.* 2010; 285: 42075-42085.
47. Farnebo L, Shahangian A, Lee Y, Shin JH, Scheeren FA, Sunwoo JB. Targeting Toll-like receptor 2 inhibits growth of head and neck squamous cell carcinoma. *Oncotarget.* 2015; 6: 9897-9907.
48. Polyak K, Kato JY, Solomon MJ, Sherr CJ, Massague J, Roberts JM, Koff A. p27Kip1, a cyclin-Cdk inhibitor, links transforming growth factor-beta and contact inhibition to cell cycle arrest. *Genes Dev.* 1994; 8: 9-22.
49. Kamesaki H, Nishizawa K, Michaud GY, Cossman J, Kiyono T. TGF-beta 1 induces the cyclin-dependent kinase inhibitor p27Kip1 mRNA and protein in murine B cells. *J Immunol.* 1998; 160: 770-7.

Table 1 Results of immunohistochemical staining of human lung cancer

Positive proportion	ADC	SCC	SCLC
51–100%	17/30 (56.7%)	10/17 (58.8%)	7/15 (46.7%)
26–50%	3/30 (10.0%)	3/17 (17.6%)	2/15 (13.3%)
0–25%	10/30 (33.3%)	4/17 (23.5%)	6/15 (40.0%)

ADC, adenocarcinoma; SCC, squamous cell carcinoma; SCLC, small cell lung carcinoma

Supplemental Table 1 Antibodies used for IHC and WB analysis

Primary antibody	Manufacturer (location)	IHC	WB
TSK (NBP1-87959)	Novus (Littleton, CO)	1:50	1:1000
Flag M2 (F1804)	Sigma Aldrich (Oakville, Canada)		1:1000
E-cadherin (610181)	BD Biosciences Pharmingen (San Jose, CA)		1:5000
Slug (C19G7)	Cell Signaling (Danvers, MA)		1:1000
Snail (C15D3)	Cell Signaling		1:500
Vimentin (E-5)	Santa Cruz Biotechnology (Santa Cruz, CA)		1:5000
p38MAPK (9212)	Cell Signaling		1:2000
P-p38MAPK (9211S)	Cell Signaling		1:2000
Erk1/2 (9102)	Cell Signaling		1:1000
P-Erk1/2 (9101S)	Cell Signaling		1:1000
P-Histone H3 (Ser10)	Millipore (Billerica, MA)		1:500
c-Myc	Cell Signaling		1:1000
β -actin (A-5441)	Sigma Aldrich		1:10000
Ki67	Dako (Tokyo, Japan)	1:50	

TSK, Tsukushi; MAPK, mitogen-activated protein kinase; Erk, extracellular signal-regulated kinase; P, phosphorylated, WB, western blotting; IHC, immunohistochemistry

Supplemental Table 2 List of primers used in PCR

Target	Sequence	Product size (bp)
TSK	F: 5'-AACCTGCTCACCAGCATCTC-3' R: 5'-GTCGTGAAGGCAGACTGA-3'	179
SNAI1	F: 5'-TTTACCTTCCAGCAGCCCTA-3' R: 5'-CCCACTGTCCTCATCTGACA-3'	207
SNAI2	F: 5'-CTTTTTCTTGCCCTCACTGC-3' R: 5'-ACAGCAGCCAGATTCCTCAT-3'	161
VIM	F: 5'-GAGAACTTTGCCGTTGAAGC-3' R: 5'-TCCAGCAGCTTCCTGTAGGT-3'	170
CDH1	F: 5'-TGCCCAGAAAATGAAAAAGG-3' R: 5'-GTGTATGTGGCAATGCGTTC-3'	200
CDH2	F: 5'-GACAATGCCCTCAAGTGTT-3' R: 5'-CCATTAAGCCGAGTGATGGT-3'	179
PODXL	F: 5'-GAGCAGTCAAAGCCACCTTC-3' R: 5'-TGGTCCCCTAGCTTCATGTC-3'	199
TGF- β 1	F: 5'-GGGACTATCCACCTGCAAGA-3' R: 5'-CCTCCTTGGCGTAGTAGTCG-3'	239
GAPDH	F: 5'-CAGCCTCAAGATCATCAGCA-3' R: 5'-TGTGGTCATGAGTCCTTCCA-3'	106
TSK (RT-PCR)	F: 5'-ATGCTTCCCCGGGTGCCAAT-3' R: 5'-GGGAGAGGTCCACGTGTAGT-3'	440
DCN (RT-PCR)	F: 5'-AATTGAAAATGGGGCTTTCC-3' R: 5'-GAGCCATTGTCAACAGCAGA-3'	222
BGN (RT-PCR)	F: 5'-GGACTCTGTCACACCCACCT-3' R: 5'-GAGCCATTGTCAACAGCAGA-3'	159
LUM (RT-PCR)	F: 5'-CAGACTGCCTTCTGGTCTCC-3' R: 5'-AGCTCAACCAGGGATGACAC-3'	186
ASPN (RT-PCR)	F: 5'-TCCCAACCAACATTCCATTT-3' R: 5'-CCTTCGCAACTTCTTTGTGG-3'	176
PODN (RT-PCR)	F: 5'-CCTCATCCTGTCCAGCAACT-3' R: 5'-GCTTCCAGAAGGTCTCGTTG-3'	197

TSK, Tsukushi; SNAI1, snail family transcriptional repressor 1; SNAI2, snail family transcriptional repressor 2; VIM, vimentin; CDH1, cadherin 1; CDH2, cadherin 2; PODXL, podocalyxin like; TGF- β 1, transforming growth factor- β 1; GAPDH, glyceraldehyde-3-phosphate dehydrogenase; DCN, decorin; BGN, biglycan; LUM, lumican; ASPN, asporin; PODN, podocan; F, forward; R, reverse

Figure legends

Fig. 1 Lung cancer tissues and cell lines highly expressing Tsukushi (TSK). (A)

Immunohistochemical staining for TSK was performed in 30 adenocarcinoma (ADC), 17 squamous cell carcinoma (SCC), and 15 small cell lung carcinoma (SCLC) specimens that had been surgically resected. TSK was detected in all of the histological types of lung cancer, especially ADC and SCC.

Representative images of each histological type are shown, and intracytoplasmic granular staining was seen. Scale bar = 50 μm . (B) Reverse transcription polymerase chain reaction analysis

(RT-PCR) was conducted using the lung cancer cell lines, including ADC, SCC, and SCLC.

Expression of small leucine-rich repeat proteoglycan (SLRP) family mRNAs, including TSK, decorin (DCN), biglycan (BGN), lumican (LUM), asporin (ASPN), and podocan (PODN), in lung

cancer cell lines. TSK mRNA was expressed in all the lung cancer cell lines examined. DCN, ASPN, and PODN mRNAs were not expressed in the lung cancer cell lines examined. BGN mRNA was

expressed in H226, H69, and H69AR cell lines. LUM mRNA was expressed in H358 and SCLC cell lines. Glyceraldehyde-3-phosphate dehydrogenase (GAPDH) used as an internal control in RT-PCR.

Fig. 2 Modification of TSK expression in H1975 adenocarcinoma cells. (A) Western blotting

(WB) analysis showed that TSK and Flag were more highly expressed in TSK-overexpressing

(TSK-OE) H1975 cell clone #2 than in clone #1. (B) FPKM levels of TSK obtained by RNA

sequence analysis and the relative expression of TSK obtained by quantitative real-time polymerase chain reaction (qRT-PCR) in TSK-OE clone #2. This result showed that TSK mRNA levels increased in TSK-OE clone #2. (C) Reverse transcription polymerase chain reaction analysis (RT-PCR) showed that TSK mRNA was not detected in TSK knockout (TSK-KO) H1975 cell clones #1 and #3, and TSK mRNA was detected at a different position in TSK-KO clone #2. (D) FPKM levels of TSK obtained by RNA sequence analysis and relative expression of TSK obtained by qRT-PCR in TSK-KO clone #2. This result showed that TSK mRNA decreased in TSK-KO clone #1. β -actin was used as an internal control for WB analysis. Glyceraldehyde-3-phosphate dehydrogenase (GAPDH) was used as an internal control for RT-PCR and qRT-PCR. Data are given as means \pm SD (B and D). *** $p < 0.001$.

Fig. 3 RNA sequence and GO analysis. (A) Venn diagrams shows the number of genes with significant differential expression levels. Comparison of the analysis of TSK-overexpressing (TSK-OE) H1975 cells and TSK knockout (TSK-KO) H1975 cell identified 94 common significant genes. (B) Four genes that were up-regulated in TSK-OE and down-regulated in TSK-KO cells lines are shown (left). Ten genes that were down-regulated in TSK-OE and up-regulated in TSK-KO cell lines are shown (right). (C) FPKM levels of TGF- β 1 and PODXL obtained by RNA sequence analysis and relative expression of these genes obtained by quantitative real-time polymerase chain

reaction (qRT-PCR) in TSK-OE cell lines (upper side). FPKM levels of these genes obtained by RNA sequence analysis and relative expression of these genes obtained by qRT-PCR in the TSK-KO (lower side). PODXL and TGF- β 1 levels were elevated in TSK-KO cell lines, but their levels were reduced in TSK-OE cell lines. Glyceraldehyde-3-phosphate dehydrogenase (GAPDH) was used as an internal control in qRT-PCR. Data are given as means \pm SD (C). * $p < 0.05$. ** $p < 0.01$.

Fig. 4 TSK regulates EMT in H1975 adenocarcinoma cells. (A) FPKM levels and relative expression of molecules related to the EMT, including cadherin-1 (CDH1), snail family transcriptional repressor 1 (SNAI1), snail family transcriptional repressor 2 (SNAI2), and vimentin (VIM) in TSK-overexpressing (TSK-OE) cell lines. Expression of SNAI1, SNAI2, and VIM was significantly reduced, but expression of CDH1 was elevated. (B) The significant reduction of SNAI1, SNAI2, and VIM in TSK-OE cell lines was detected by western blotting (WB). However, induction of CDH1 was not evident. (C) FPKM levels and relative expression of the EMT-related molecules, including CDH1, SNAI1, SNAI2, and VIM in TSK knockout (TSK-KO) cell lines. Expression of SNAI2 and VIM was significantly elevated, but expression of SNAI1 was reduced. (D) Induction of SNAI1, SNAI2, VIM, and CDH1 was not evident by WB. (E) The degree of cell invasion in TSK-OE cell lines was clearly less than that of the mock. Scale bar = 200 μ m. β -actin was used as an internal control in WB analysis. Glyceraldehyde-3-phosphate dehydrogenase (GAPDH) was used as

an internal control in qRT-PCR. Data are given as means \pm SD (A, C and E). * $p < 0.05$. ** $p < 0.01$.

*** $p < 0.001$.

Fig. 5 TSK is involved in cell proliferation in H1975 adenocarcinoma cells. (A) Cell counting

assays revealed that TSK overexpression enhanced the proliferation of H1975 adenocarcinoma cells.

(B) Western blotting (WB) analysis revealed that mitogen-activated protein kinase (MAPK) was not

activated in TSK-overexpressing (TSK-OE) cell lines. (C) The mock transfected and TSK-OE cell

lines were injected subcutaneously into the backs of four each of Rag2 and Jak3 double gene

deficient mice. After 20 days, the tumors were removed and measured. The size of xenotransplanted

tumors from the TSK-OE cell lines were significantly larger than that from mock transfected cell

lines. Scale bar = 10 mm. (D) hematoxylin and eosin (H&E) staining and immunostaining for TSK

and Ki67 in the xenotransplanted tumors from mock transfected and TSK-OE cell lines. Staining

intensity for TSK and Ki67-labeling index were elevated in tumor tissues from TSK-OE cell lines,

compared with from mock transfected cell lines. Scale bar = 50 μ m. (E) Western blotting analysis

revealed that MAPK, P-Histone H3, and c-myc levels were not enhanced in the TSK-OE cell lines.

β -actin was used as an internal control in WB analysis. Data are given as means \pm SD (A, C and D).

* $p < 0.05$. ** $p < 0.01$.

Supplemental Fig. 1 Biological process and molecular function by gene ontology analysis of significant genes obtained by RNA sequence analysis. The top 20 significantly enriched terms are shown in the graph.

Supplemental Fig. 2 Heatmap of the FPKM of significant genes obtained by RNA sequence analysis annotated to the ontologies related to adhesion and proliferation. In the common significant genes, NRP2 and PODXL appear adhesion-related molecules and PCSK1N and EDNRA appear as proliferation-related molecules.

Figure 1

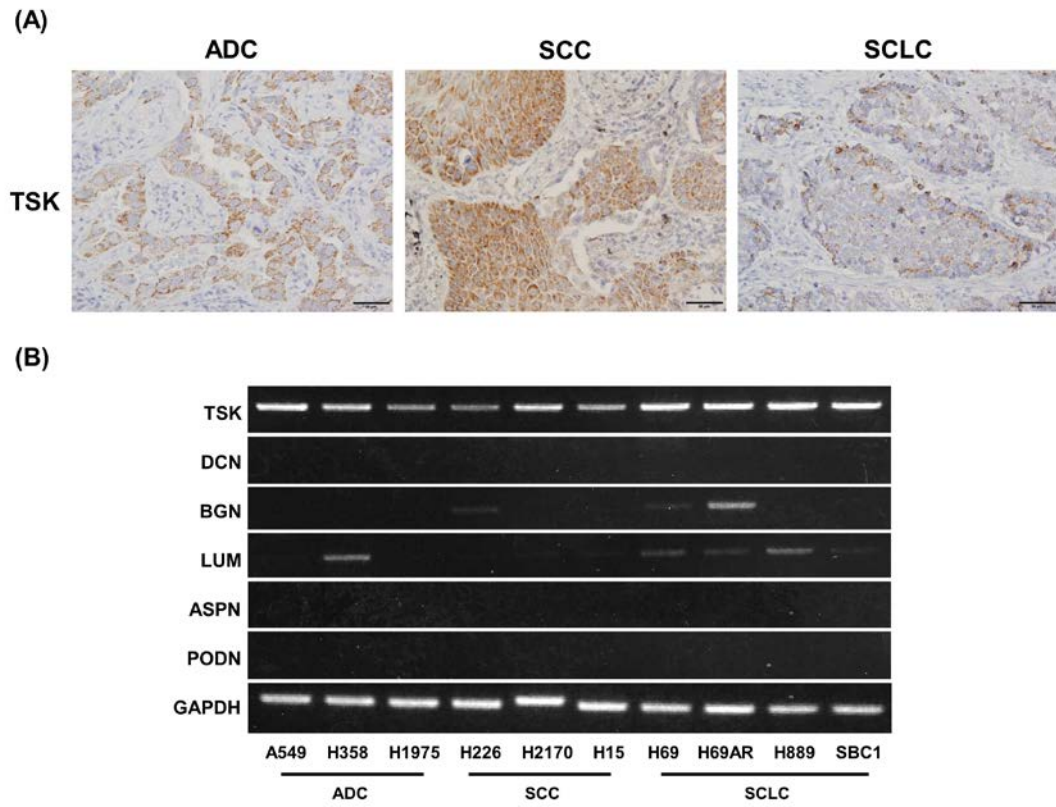


Figure 2

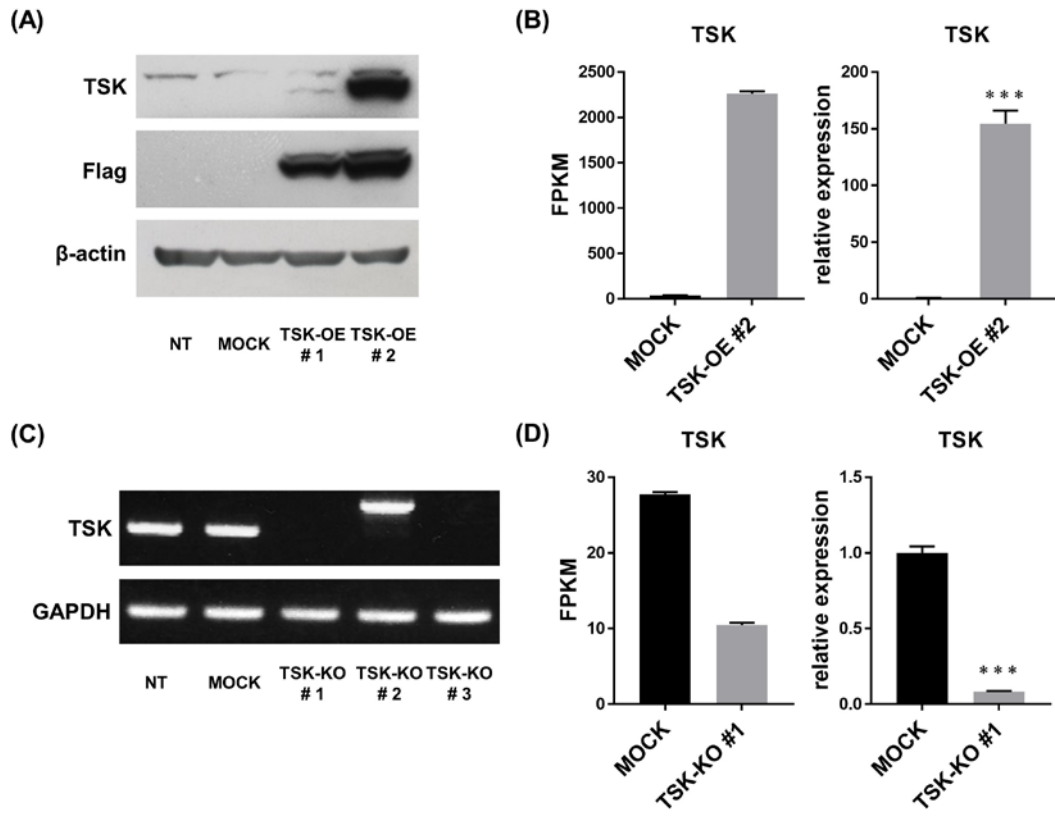


Figure 3

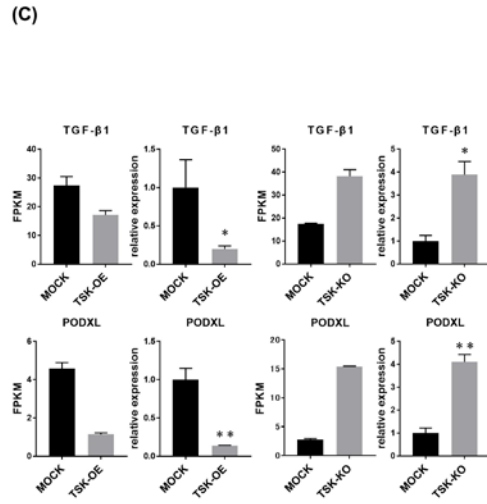
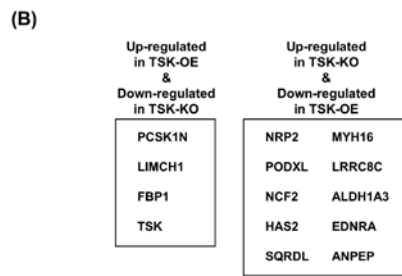
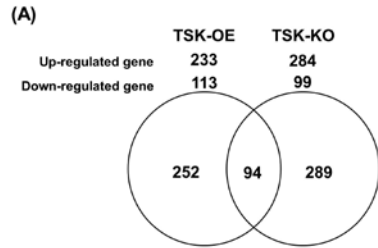


Figure 4

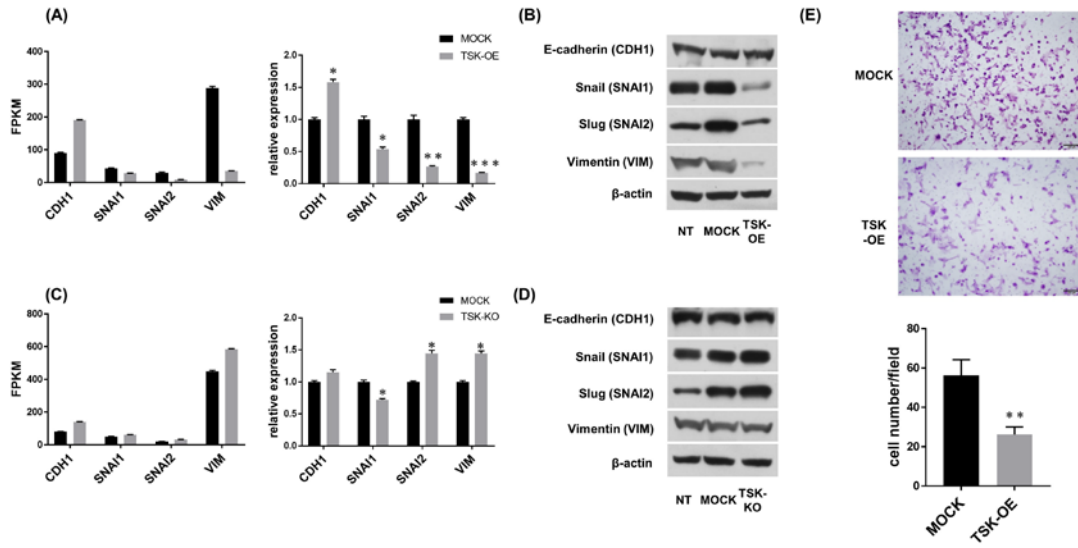
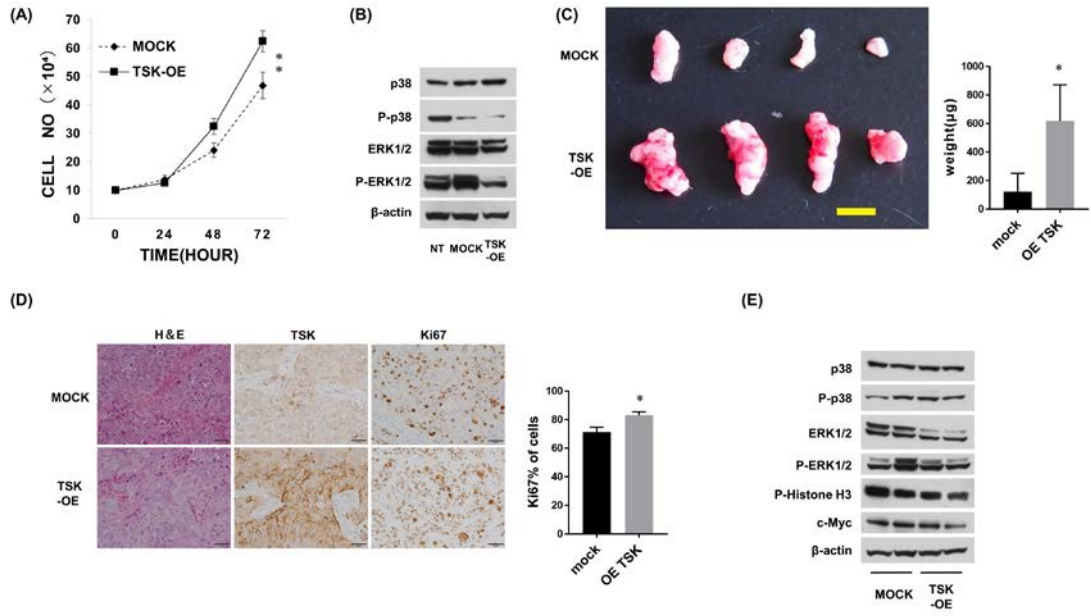
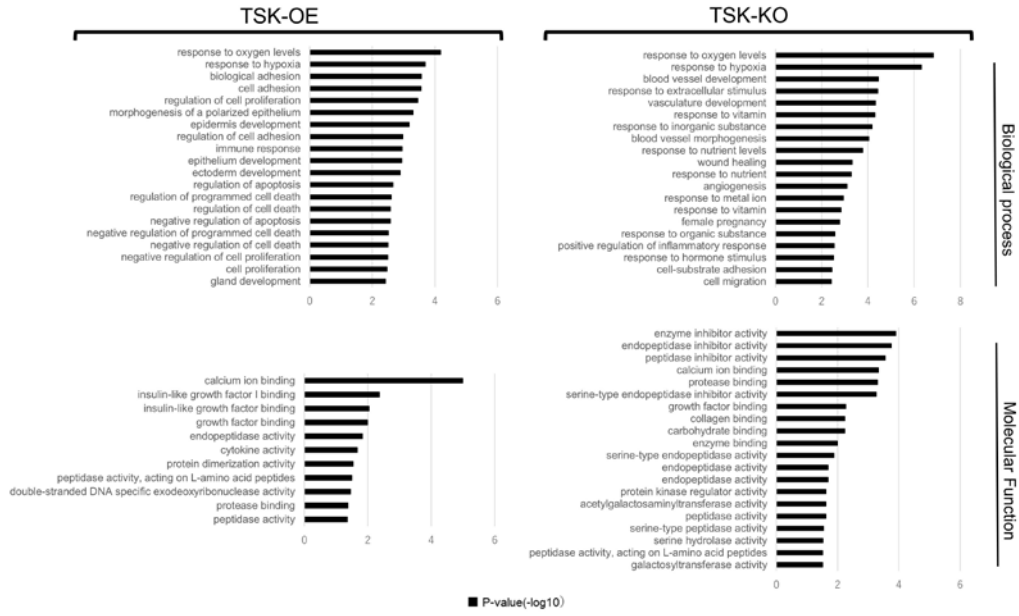


Figure 5



Supplemental Figure 1



Supplemental Figure 1

